Proceeding of the IEEE
International Conference on Robotics and Biomimetics
Dali, China, December 2019

Compliance Control of the Hydraulic-Driven Single Legged Robot

Yixiao Fan, Xu Li, Haibo Feng, Songyuan Zhang, Chengbo Zhang and Yili Fu

Abstract— **This paper presents the force control strategies and a kind of compliance control strategies of the hydraulic-driven unit (HDU) in the legged robots. The model of HDU is established and the transfer function of the HDU force control system is given. The analysis of the force control strategies is introduced according to the characteristic of the HDU system. Based on the force control strategy called velocity feedback control strategy which performs the best, the virtual model control strategy which is a kind of compliance control strategy is presented to enhance the adaptability of the legged robot. Finally, the experiments are taken on the HDU experiment platform to test the performance of the force control strategies and the compliance control strategy. The landing buffer experiments are taken on the single leg robot to verify the effectiveness of the compliance control strategy. In the landing buffer experiments, the impact force of the single leg robot's knee HDU is about 0.33 time of what it is without the compliance control strategy while landing.**

I. Introduction

Footed robot is a kind of bionic robot that mimic the structure of human being. This kind of robot can adapt to almost all the environment, so it is particularly suitable for the missions in the field. This structure also provides the robot the ability to jump a certain high which shows a great mobility in order to avoid obstacles on the ground [1]. Many legged robots have been developed Because of their advantages. Italian Institute of Technology (IIT) developed a quadruped hydraulic-driven robot called HyQ [2]. Boston Dynamic successively developed many hydraulic legged robots one after another like Petman [3], Bigdog [4], Cheetah [5] and multiple generations of Atlas [6].

Most of the hydraulic robots are biped or quadruped. Researchers have designed different types of hydraulic robot which can walk stably. Some splendid ones can even be used in the complicated environments carrying some load. The hydraulic-driven system of the robot consists of the hydraulic cylinders and the sensors. There are plenty of advantages of the hydraulic actuator like fast response speed, large output power and great anti-interference ability. But it's disadvantages like system nonlinearity, model inaccuracy and parameter uncertainty limit its applications in the field of legged robot. Therefore, various control strategies have been studied to obtain better performance under these disadvantages. Zhu and Piedboeu proposed an adaptive output force tracking control strategy based on virtual decomposition control for the hydraulic cylinders [7]. Koivumaki and Mattila proposed a control strategy based on virtual decomposition control for 2-DOF heavy-duty hydraulic actuators [8]. Kim proposed a stable and reliable control strategy based on lyapunov method for hydraulic parallel manipulator SGF [9,10]. Pi and Wang [11] proposed a cascade control method applied to the joint space of a 6-DOF parallel hydraulic manipulator.

For the reason that the impact always occurs when the robot contacts the environment, it is important to enhance the robot's ability of environmental adaptation which makes the compliance control strategy become vital. Now there are two mainstream compliance control strategies that are passive compliance strategy and active compliance strategy [12]. The passive compliance strategy is performed by elastic elements like spring and rubber to absorb the impact force[13]. The most famous passive compliant actuator must be SEA which was introduced by Pratt[14]. It can absorb the impact well and can be applied in many situations. But its adaptability is poor because the system stiffness is determined by the spring stiffness.

However, passive compliance strategy has difficulties in control so it is only suitable for impact mitigation in a simple way and has poor adaptability to complex environment. In order to overcome the disadvantages of passive compliance strategy, researchers became interested in active compliance strategy[15].The common active compliance control methods include impedance control [16], operation space control [17], hybrid force-position control [18] and virtual model control. IIT applied a low-level force control based on feedback linearization technique in hydraulic legged robot HyQ[19]. Michele proposed a design method of the joint impedance controller based on internal torque loop and positive velocity feedback loop [20].

The compliance system has the ability to make the actuator adapt to the impact force from the environment in order to reduce the mechanical structure damage of the robot. Active compliance control has better adaptability to enable the robots to adjust themselves according to the environment which allows the robot to walk more stably, perform missions on a more complex terrain.

This paper is organized as follows: Section II briefly introduces the model establishment of the HDU's force control system. Section III presents the control strategies of HDU. Section IV depicts the experiments of the HDU's force control strategies and the single leg robot's virtual model control while landing.

Research supported by the Foundation for Innovative Research Groups of the National Natural Science Foundation of China (Grant No.51521003).(corresponding author:Yili Fu and Haibo Feng)*

Yixiao Fan, Xu Li, Haibo Feng, Songyuan Zhang, Chengbo Zhang and Yili Fu are with State Key Laboratory of Robotics and System, Harbin Institute of Technology, Harbin, Heilongjiang Province, 150001, China, fax: +86-0451-86414422; moshouzhengba_la@126.com, hitlx@hit.edu.cn, haibo_feng@hotmail.com, zhangsy@hit.edu.cn, zcbo96@163.com, meylfu@hit.edu.cn

978-1-7281-6321-5/19//$31.00 ©2019 IEEE

II. Modeling of HDU's Force Control System

In this section, each part of HDU is modeled and the model of HDU's force control system is established. After that the model is analysed and the transfer function is given.

The HDU consists of a flow servo valve, a hydraulic cylinder and sensors, as shown in Fig. 1. The piston can make reciprocating motion due to the hydraulic oil controlled by the servo valve.

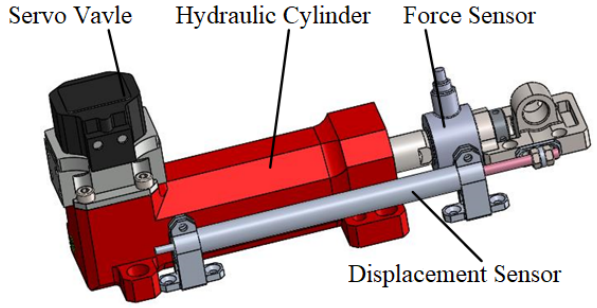

Fig. 1. The 3D model of HDU

In practical engineering applications, the relationship between the current and the voltage is usually considered as direct ratio. The transfer function is:

$$\frac{I}{E_\varepsilon} = K_a \tag{1}$$

Where K_a is the potentiometer scaling factor, I is the servo valve current, E_ε is the voltage.

The transfer function of the servo valve here is considered as a proportional link because the servo valve's inherent frequency is much bigger than the hydraulic system's, so the transfer function can be expressed as

$$W_{sv}(s) = \frac{x_v}{I} = K_{sv} \tag{2}$$

Where x_v is the valve core displacement, K_{sv} is the gain of the servo valve.

The relationship between the voltage and the displacement of the displacement sensor is

$$\frac{U_Y}{Y} = K_Y \tag{3}$$

Where U_Y is the displacement sensor's voltage, Y is the displacement sensor's displacement, K_Y is the displacement sensor's gain.

The relationship between the voltage and the force of the force sensor is

$$\frac{U_F}{F} = K_F \tag{4}$$

Where U_F is the force sensor's voltage, F is the force sensor's force, K_F is the force sensor's gain.

Considering the transfer functions above and the linear equation of the servo valve flow, the flow continuity equation and the force equilibrium equation below,

$$\begin{cases} Q_L = K_q x_v - K_c p_L \\ Q_L = A_1 \dot{x}_p + \frac{V_t}{2(1+n^2)\beta_e} \dot{p}_L \\ F_g = p_1 A_1 - p_2 A_2 = A_1 p_L = m_t \ddot{x}_p + B\dot{x}_p + K x_p \end{cases} \tag{5}$$

Where $Q_L = \frac{Q_1 + nQ_2}{1+n^2}$, Q_1 is the rodless cavity flow, Q_2 is the rod cavity flow, K_q is the servo valve's flow gain, K_c is the servo valve's flow-pressure coefficient, $n = \frac{A_2}{A_1}$, A_1 is the effective area of the rodless cavity, A_2 is the effective area of the rod cavity, $p_L = P_1 - nP_2$, P_1 is the rodless cavity pressure, P_2 is the rod cavity pressure, x_p is the displacement of the piston, V_t is the total compression volume, β_e is the bulk elastic modulus of the hydraulic oil, m_t is the load mass, B is the load damping, K is the load stiffness.

The block diagram of the force control system is considered as Fig. 2.

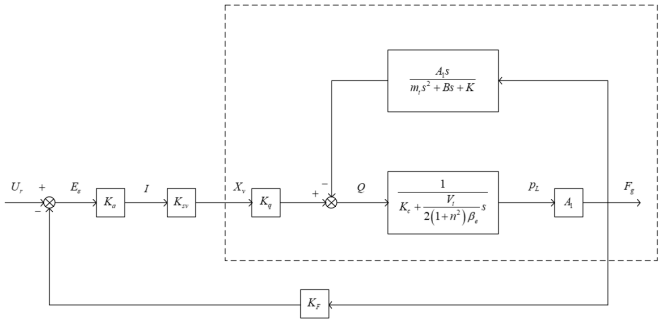

Fig. 2. The block diagram of HDU force control system

Since the load damping B is very small and the system meets the condition $\left[\frac{K_c\sqrt{Km_t}}{A_1^2(1+K/K_h)}\right]^2 << 1$, the transfer function of the system inside the dashed box can be simplified as

$$\frac{F_g}{X_v} = \frac{\frac{K_q}{K_c} A_1 \left(\frac{s^2}{\omega_m^2} + 1\right)}{\left(\frac{s}{\omega_r} + 1\right)\left(\frac{s^2}{\omega_0^2} + \frac{2\xi_0}{\omega_0} s + 1\right)} \tag{6}$$

Where ω_m is the inherent frequency of the load, $\omega_m = \sqrt{\frac{K}{m_t}}$, $\omega_r = \frac{\frac{K_c}{A_1^2}}{\frac{1}{K_h} + \frac{1}{K}}$, $\omega_0 = \omega_m\sqrt{1 + \frac{K_h}{K}}$, $\xi_0 = \frac{1}{2\omega_0} \frac{2(1+n^2)\beta_e K_c}{V_t[1+(K/K_h)]}$, K_h is the stiffness of the hydraulic spring, $K_h = \frac{2(1+n^2)A_1^2}{V_t}$.

For the reason that the hydraulic cylinder is asymmetric, when the piston sticks out ($\dot{x}_p > 0$),

$$\begin{cases} K_q = C_d w \sqrt{\frac{2}{(1+n^3)\rho}(p_s - p_L)} \\ K_c = \frac{C_d w x_v}{p_s - p_L} \sqrt{\frac{1}{2(1+n^3)\rho}(p_s - p_L)} \end{cases} \tag{7}$$

and when the piston retracts ($\dot{x}_p < 0$),

$$\begin{cases} K_q = C_d w \sqrt{\frac{2n^3}{(1+n^3)\rho}(p_s - p_L)} \\ K_c = \frac{C_d w x_v}{p_s - p_L} \sqrt{\frac{n^3}{2(1+n^3)\rho}(p_s - p_L)} \end{cases} \tag{8}$$

Where C_d is the flow coefficient of the valve port, w is the throttle area gradient, ρ is the density of the hydraulic oil, p_s is the pressure of the power unit.

The model which established in this section will be used in Section III for the design of the system controllers.

III. Force Control Strategies of HDU

In this section, HDU's force control strategies are studied based on the system model established in Section II and the simulational model is built in Matlab to verify the effectiveness of the control strategies.

A. PID Force Control Strategy

The hydraulic force control system can use the PID control strategy to control. Since the gain of the system is big, it will cause overshoot and oscillation easily. The P control is added to reduce the gain so as to prevent the system from overshooting and oscillating. For the reason that the deviation is always exist between the expected force signal and the output force signal in the force control system, the I control is needed to eliminate the offset. Due to the strong noise of the force sensor, the D control can easily lead to oscillation and destroy the stability of the system. In conclusion, PI control strategy is adopted.

The open loop transfer function of the system is

$$\frac{F_g}{U_r}=\frac{K_a K_{sv} K_F \frac{K_q}{K_c} A_1 \left(\frac{s^2}{\omega_m^2}+1\right)}{\left(\frac{s}{\omega_r}+1\right)\left(\frac{s^2}{\omega_0^2}+\frac{2\xi_0}{\omega_0}s+1\right)} \tag{9}$$

To keep the system stable, K_p can't be too big or it will lead the system into oscillation, so K_p must satisfy the condition

$$K_p < \frac{(2\xi_0+2)\left(\frac{\omega_0}{\omega_r}+1\right)}{K_a K_{sv} K_F \frac{K_q}{K_c} A_1 \left(\frac{\omega_0^2}{\omega_m^2}+1\right)} \tag{10}$$

The P control parameter K_p and the I control parameter K_I are adjusted depending on the model in simulink to make the system response better. After the adjustment the step response and the sinusoid response of the system are shown in Fig. 3 respectively.

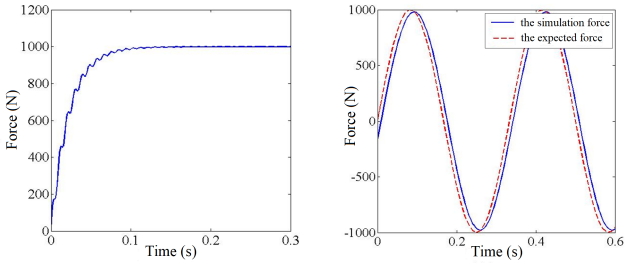

(a) Step response (b) Sinusoid response

Fig. 3. The simulation responses under PID control strategy

In the simulation, for the step response, there is almost no overshoot in the system output and the system performs a certain rapidity by becoming stable in around 0.15s. For the 3Hz sinusoid response, the maximum error between the output value and the expected value is about 3% and the phase lag is about 10 degrees which shows a good tracking performance.

B. Velocity Feedback Control Strategy

During the experiments, the HDU will generate additional flow due to the piston movement which will cause the generation of the redundant force [21]. The redundant force will narrow the system bandwidth, make the dynamic performance worse and even affect the accuracy of the system. Therefore, the redundant force is needed to be suppressed. Velocity feedback control strategy is a kind of compensation method used for suppressing the redundant force.

When $\dot{x}_p > 0$, let $K_d = C_d w \sqrt{\frac{1}{\rho}}$, the system flow equation is

$$Q_1 = K_d x_v \sqrt{\frac{2}{1+n^3}(p_s - p_L)} \tag{11}$$

Ignoring the compression and leakage of the hydraulic oil, the redundant flow caused by the load velocity is

$$Q_1 = \dot{x}_p A_1 \tag{12}$$

The output force of the hydraulic cylinder is

$$F = p_L A_1 \tag{13}$$

The relationship between the valve core displacement and the driving voltage is

$$x_v = K_a K_{sv} U \tag{14}$$

Considering (11)(12)(13)(14) together, the compensation voltage of the servo valve is

$$\Delta U = \frac{\dot{x}_p A_1}{K_a K_{sv} K_d \sqrt{\frac{2}{1+n^3}\left(p_s - \frac{F}{A_1}\right)}} \tag{15}$$

When $\dot{x}_p < 0$, the system flow equation is

$$Q_1 = K_d x_v \sqrt{\frac{2}{1+n^3}(n p_s + p_L)} \tag{16}$$

The compensation voltage can be calculated in the same way as

$$\Delta U = \frac{\dot{x}_p A_1}{K_a K_{sv} K_d \sqrt{\frac{2}{1+n^3}\left(n p_s + \frac{F}{A_1}\right)}} \tag{17}$$

Adjusting the simulation model according to the results above, the step response and the sinusoid response of the system are shown in Fig. 4 respectively.

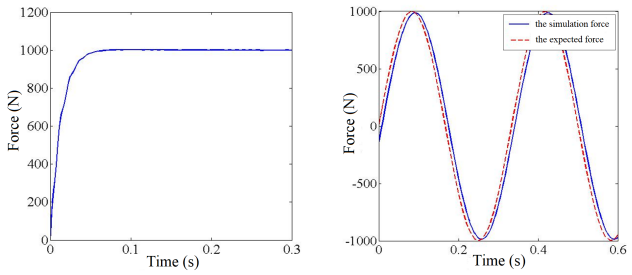

(a) Step response (b) Sinusoid response

Fig. 4. The simulation responses under velocity feedback control strategy

In the simulation, for the step response, the fluctuation has been suppressed and it takes around 0.08s to become stable. For the 3Hz sinusoidal response, the maximum error between the output value and the expected value is about 1.5% and the phase lag is about 8.7 degrees, which shows a better tracking performance.

After the addition of the velocity feedback control strategy, the system responds faster, the response error and the phase lag become smaller and the ripple phenomenon has been eliminated.

C. Virtual Model Control Strategy

For the reason that the impact force is needed to be control in order to protect the hardware of the robot while landing, the virtual model control strategy which is a kind of compliance control strategy is taken into account. The HDU virtual model is established as Fig. 5.

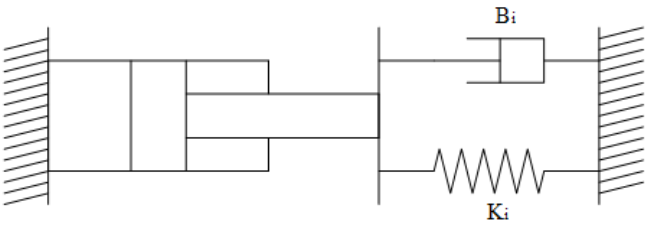

Fig. 5. HDU with virtual spring-damping model

The virtual spring-damping system is set parallelly to the rod between the rod and the environment. The HDU expected output force can be calculated as

$$F_e = K_i \left(x_p - x_{p0}\right) + B_i \dot{x}_p \tag{18}$$

Where K_i is the virtual spring stiffness, B_i is the virtual damping coefficient, x_{p0} is the expected position of the piston.

Through this output force, the piston can restore to the initial position, the amplitude of the impact can be reduced and the energy can be consumed by the virtual damping.

IV. Experiments and Results

This section shows the process of the experiments and results. The HDU experiment platform is built to evaluate the control strategies mentioned in Section III and the landing buffer experiments are performed on the single leg robot to verify the effectiveness of virtual model control strategy.

A. Experiments of HDU's Force Control Strategies

The HDU experiment platform is mainly composed of two hydraulic cylinders in series with a rigid element between them. The left hydraulic cylinder uses position control and the right one uses force control. The stroke of each is 100mm. The platform is shown in Fig. 6.

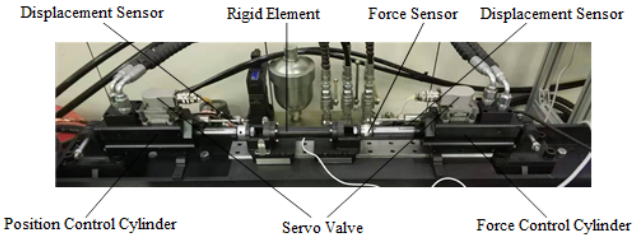

Fig. 6. HDU experiment platform

1)PID Control Experiment: The PID parameters are adjusted according to the simulation results and the supply pressure is adjusted to 5MPa. The experiment results of the response of the 1000N step signal and the 3Hz sinusoidal signal are shown in Fig. 7 respectively.

The experiment results show that the system has an overshoot about 5% and takes around 0.2s to become stable for the step signal. The amplitude attenuation is about 2% and the phase lag is about 17 degrees for the sinusoidal signal which basically achieves the requirement of force tracking though the rapidity of the system is needed to be better.

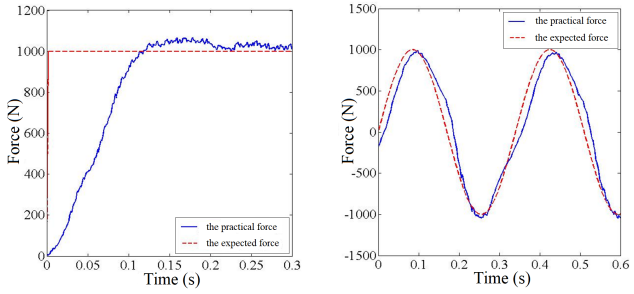

(a) Step response (b) Sinusoid response

Fig. 7. The system responses under PID control strategy

2)Velocity Feedback Control Experiment: The parameters are set according to the calculation in Section III and the supply pressure is also adjusted to 5MPa. The experiment results of the response of the 1000N step signal and the 3Hz sinusoidal signal are shown in Fig. 8 respectively.

The experiment results show that the system takes about 0.15s to become stable and has almost no overshoot for the step signal. For the sinusoidal signal, the amplitude attenuation is about 1.5% and the phase lag is about 11 degrees. Compared with PID control, the performance of the system is improved.

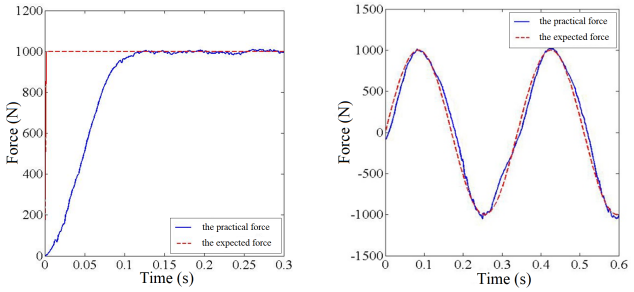

(a) Step response (b) Sinusoid response

Fig. 8. The system responses under velocity feedback control

3)Virtual Model Control Experiment: The supply pressure is set to 5MPa and the expected output force of HDU is set to 1000N. The parameters of the virtual spring-damping system are $K_i = 50N/mm$ and $B_i = 50N/(mm/s)$. The amplitudes of the external sinusoid position disturbances are 5mm and the frequency are 1Hz and 2Hz respectively. The experiment results are shown in Fig. 9.

As the experiment results, it meets the expected system requirement that the output force will change according to the position disturbance. The higher the frequency of the position disturbance is, the worse the system tracking ability is.

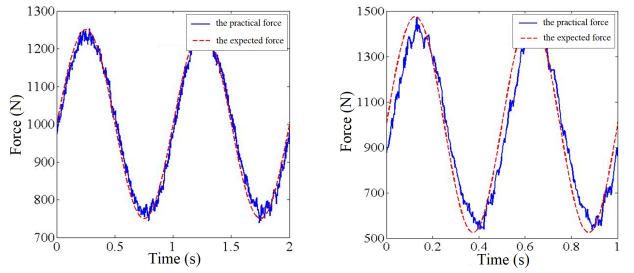

(a) 1Hz disturbance response (b) 2Hz disturbance response

Fig. 9. The system responses under velocity feedback control

B. The Single Leg Robot landing buffer experiment

Fig. 10. Picture of the single leg robot fixed to a vertical slider

The single leg robot is shown in Fig. 10. Adjusting the supply pressure to 7MPa and setting the initial angle of the knee to 130 degrees, the single leg robot will be dropped from the height of 100mm. The force of the knee HDU and the hip HDU while landing without buffer strategy are shown in Fig. 11 respectively.

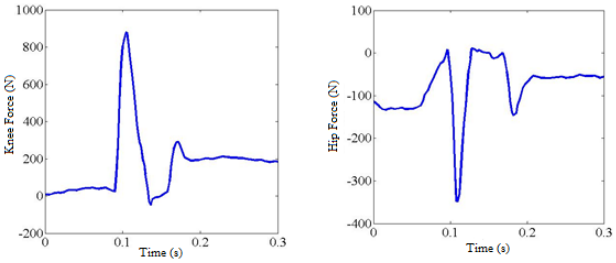

(a) Knee HDU force (b) Hip HDU force

Fig. 11. The output force of the joints' HDU without buffer strategy

The virtual model strategy is added into the landing control system to compare with the landing without buffer strategy. Adjusting the supply pressure to 7MPa and setting the initial angle of the knee to 130 degrees, the parameters of the knee HDU virtual model system are K_{ik}= 150N/mm, B_{ik}= 1.5N · s/mm and the parameters of the hip are K_{ih}= 150N/mm, B_{ih}= 0.5N · s/mm. Dropping the robot from the height of 100mm, the results are shown in Fig. 12.

The experiment results show that the maximum impact force of the knee and hip are 900N and 350N respectively without buffer strategy and after the rebound the maximum force of the knee and hip are 300N and 150N respectively which appears 0.06s later after the first peak. After the addition of the virtual model control, the maximum impact force of the knee and hip are reduced to 320N and 230N respectively and the rebound is suppressed which indicate the effectiveness of the virtual model control.

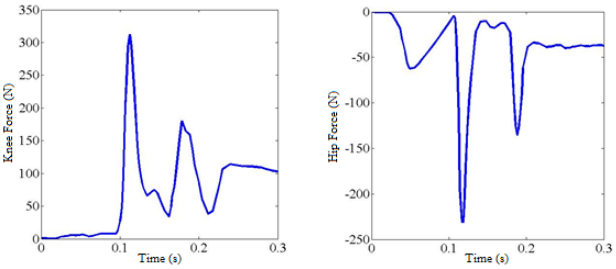

(a) Knee HDU force (b) Hip HDU force

Fig. 12. The output force of the joints' HDU under virtual model control

V. Conclusions and Future Work

This paper presents the PID control strategy, velocity feedback control strategy and virtual model control strategy of HDU in the legged robot's joint. The model of HDU is established and the transfer function of HDU's force control system is given. PID control strategy and velocity feedback control strategy are used to design the system

controller. After the simulation, the experiments of these two control strategies are taken on the HDU platform to test their performance. The velocity feedback control strategy which performs better is used in the virtual model control strategy. The virtual model control is applied on the HDU platform to verify its effectiveness and the single leg robot to test its performance on landing buffer.

There is an impact force exists when the hydraulic cylinder switches its direction of movement. The reason is that the asymmetric hydraulic cylinder is controlled by the symmetric valve. The performance may be better by using an asymmetric valve to control the asymmetric hydraulic cylinder.

ACKNOWLEDGMENT

The authors would like to thank the Foundation for Innovative Research Groups of the National Natural Science Foundation of China (Grant No.51521003), Heilongjiang Postdoctoral Scientific Research Foundation (LBH-Q17068), the self-managed project of the State Key Laboratory of Robotics and System in Harbin Institute of Technology (SKLRS201801A01, SKLRS201801A02).

REFERENCES

[1] Kovac, M., Fuchs, M., Guignard, A., Zufferey, J. C., Floreano, D. 2008, May. A miniature 7g jumping robot. In *2008 IEEE International Conference on Robotics and Automation* pp. 373-378. IEEE.

[2] Semini, C. (2010). HyQ-design and development of a hydraulically actuated quadruped robot. Doctor of Philosophy (Ph. D.), University of Genoa, Italy.

[3] Nelson, G., Saunders, A., Neville, N., Swilling, B., Bondaryk, J., Billings, D., Raibert, M. (2012). Petman: A humanoid robot for testing chemical protective clothing. *Journal of the Robotics Society of Japan*, 30(4), 372-377..

[4] Raibert, M., Blankespoor, K., Nelson, G., Playter, R. (2008). Bigdog, the rough-terrain quadruped robot. *IFAC Proceedings Volumes*, 41(2), 10822-10825.

[5] Li, Y., Li, B., Ruan, J., Rong, X. (2011, September). Research of mammal bionic quadruped robots: A review. In *2011 IEEE 5th International Conference on Robotics*, Automation and Mechatronics (RAM) pp. 166-171. IEEE.

[6] de Waard, M., Inja, M., Visser, A. 2013, April. Analysis of flat terrain for the atlas robot. In *2013 3rd Joint Conference of AI & Robotics and 5th RoboCup Iran Open International Symposium* pp. 1-6. IEEE.

[7] Zhu, W. H., Dupuis, E., Piedboeuf, J. C. 2004, June. Adaptive output force tracking control of hydraulic cylinders. In *Proceedings of the 2004 American Control Conference* Vol. 6, pp. 5066-5071. IEEE.

[8] Koivumäki, J., Mattila, J. 2013, July. The automation of multi degree of freedom hydraulic crane by using virtual decomposition control. In *2013 IEEE/ASME International Conference on Advanced Intelligent Mechatronics* pp. 912-919. IEEE.

[9] Kim, D. H., Kang, J. Y., Lee, K. I. (2000). Robust tracking control design for a 6 DOF parallel manipulator. *Journal of Robotic Systems*, 17(10), 527-547.

[10] Dasgupta, B., Mruthyunjaya, T. S. (2000). The Stewart platform manipulator: a review. *Mechanism and machine theory*, 35(1), 15-40.

[11] Pi, Y., Wang, X. (2010). Observer-based cascade control of a 6-DOF parallel hydraulic manipulator in joint space coordinate. *Mechatronics*, 20(6), 648-655.

[12] Xu Li, Haibo Feng, Songyuan Zhang, Haitao Zhou, Yixiao Fan, Zhennan Wang and Yili Fu. 2019 July. Vertical Jump Control of Hydraulic Single Legged Robot (HSLR). In *Proceedings of the 2019 IEEE/ASME International Conference on Advanced Intelligent Mechatronics*, pp. 1421-1427

[13] X. Li, H. T. Zhou, H. B. Feng, S. Y. Zhang and Y. L. Fu, "Design and Experiments of a Novel Hydraulic Wheel-legged Robot (WLR)," in *Intelligent Robots and Systems (IROS 2018)*, 2018 IEEE/RSJ International Conference on, pp. 3292-3297, 2018.

[14] Robinson, D. W., Pratt, J. E., Paluska, D. J., Pratt, G. A. (1999, September). Series elastic actuator development for a biomimetic walking robot. In *1999 IEEE/ASME International Conference on Advanced Intelligent Mechatronics* (Cat. No. 99TH8399) pp. 561-568. IEEE.

[15] Li, X., He, J., Feng, H., Zhou, H., Fu, Y. (2018, December). Research on Compliance Control for the single Joint of a Hydraulic Legged Robot. In *2018 IEEE International Conference on Robotics and Biomimetics (ROBIO)* pp. 1720-1726. IEEE.

[16] Hogan, N. (1984, June). Impedance control: An approach to manipulation. In *1984 American control conference* pp. 304-313. IEEE.

[17] Khatib, O. (1987). A unified approach for motion and force control of robot manipulators: The operational space formulation. *IEEE Journal on Robotics and Automation*, 3(1), 43-53.

[18] Raibert, M. H., Craig, J. J. (1981). Hybrid position/force control of manipulators. *Journal of dynamic systems, measurement, and control*, 103(2), 126-133.

[19] Boaventura, T., Semini, C., Buchli, J., Frigerio, M., Focchi, M., Caldwell, D. G. (2012, May). Dynamic torque control of a hydraulic quadruped robot. In *2012 IEEE international conference on robotics and automation* pp. 1889-1894. IEEE.

[20] Focchi, M., Medrano-Cerda, G. A., Boaventura, T., Frigerio, M., Semini, C., Buchli, J., Caldwell, D. G. (2016). Robot impedance control and passivity analysis with inner torque and velocity feedback loops. *Control Theory and Technology*, 14(2), 97-112.

[21] Feng, Q., Xiaoqiang, G., Bo, Y., Zhongcai, P. (2011, August). Theoretical analysis of surplus torque in electro-hydraulic load simulator. In *Proceedings of 2011 International Conference on Fluid Power and Mechatronics* pp. 150-153. IEEE.